Cascaded entanglement enhancement

Zhihui Yan (闫智辉), Xiaojun Jia (贾晓军), Xiaolong Su (苏晓龙), Zhiyuan Duan (段志园), Changde Xie (谢常德), and Kunchi Peng (彭堃墀)

Phys. Rev. A **85**, 040305 — Published 16 April 2012

DOI: 10.1103/PhysRevA.85.040305

Cascaded Entanglement Enhancement

Zhihui Yan(闫智辉), Xiaojun Jia(贾晓军),* Xiaolong Su(苏晓龙),
Zhiyuan Duan(段志园), Changde Xie(谢常德), and Kunchi Peng(彭堃墀)

State Key Laboratory of Quantum Optics and Quantum Optics Devices,
Institute of Opto-Electronics, Shanxi University, Taiyuan, 030006, P. R. China

We present a cascaded system consisting of three non-degenerate optical parametric amplifiers (NOPAs) for the generation and the enhancement of quantum entanglement of continuous variables. The entanglement of optical fields produced by the first NOPA is successively enhanced by the second and the third NOPAs from $-5.3\ dB$ to $-8.1\ dB$ below the quantum noise limit. The dependence of the enhanced entanglement on the physical parameters of the NOPAs and the reachable entanglement limitation for a given cascaded NOPA system are calculated. The calculation results are in good agreement with the experimental measurements.

PACS numbers: 03.67.Bg, 42.50.Dv, 03.65.Ud, 42.50.Lc

* jiaxj@sxu.edu.cn

Nonlocal quantum entanglement is the key resource to realize quantum information processing (QIP) [1–3]. The entangled states of single photons (qubits) and optical modes (qumodes) have been applied in QIP with discrete and continuous variable (DV and CV) regimes, respectively [4, 5]. The Einstein-Podolsky-Rosen (EPR) [6] entangled states of optical field are the essential quantum resources for implementing CV QIP. In the quantum optics the quadrature-amplitude and the quadrature-phase play the roles of the canonical position and momentum variables in the original EPR proposal [7]. The optical EPR state is a two-mode entangled state consisting of two sub-modes with quantum correlations between both quadrature-amplitude and quadrature-phase. If the experimentally measured combination of the fluctuation variances for the amplitude sum (difference) and the phase difference (sum) of the two sub-modes is smaller than the corresponding quantum noise limit (QNL), the two optical sub-modes are inseparable and thus form an optical state with EPR entanglement [7–9]. The quadrature squeezed states of light are the necessary base to establish quantum entanglement among optical fields [10]. A scheme of generating CV optical entangled states is to interfere two single-mode squeezed states of light with an identical frequency and a constant phase-difference on a $50/50$ beamsplitter [5, 11]. The two single-mode squeezed states are often produced by a pair of degenerate optical parametric amplifiers (DOPAs) with identical type-I nonlinear crystal pumped by a laser to ensure high interference efficiency. Through carefully technical improvement on suppressing the phase fluctuation of optical field and reducing the intra-cavity losses of DOPA, the squeezing level of the single-mode squeezed states is continually renewed in recent years [12–16]. So far, the squeezing over $-12\ dB$ below QNL has been achieved by a group in Hannover [13, 15]. Coupling a single-mode squeezed state of -9.9 dB and a vacuum field on a $50/50$ beam splitter, the EPR entangled state of light with the quantum correlation of amplitude and phase quadratures of $-3\ dB$ below the QNL was obtained in 2011 [16]. The four-mode CV entanglement of $-6\ dB$ below the QNL was achieved by combining four initial single-mode squeezed states generated by four DOPAs [17].

Another important device to generate CV EPR entangled state of optical field is the non-degenerate optical parametric amplifier (NOPA) consisting of an optical cavity and a type-II nonlinear crystal. Through the intra-cavity frequency-down conversion process in a NOPA, a pair of non-degenerate optical modes with amplitude and phase quadrature correlations is directly produced, which is an EPR entangled state [18–20]. Twenty years ago, Kimble's group experimentally generated a pair of CV entangled optical beams with a NOPA and demonstrated the EPR paradox firstly in CV regime [18]. Then, NOPAs operating at different version (above or lower

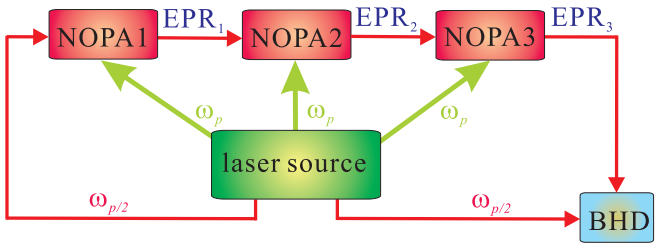

FIG. 1. (Color online) The principle schematic of the cascaded entanglement enhancement system.

the threshold, amplification or de-amplification) are used as the sources of generating optical CV entangled states and the produced EPR beams are applied in a variety of CV QIP experiments [19–24]. However, in a long period the EPR entanglement level was kept around $-4\ dB$ or lower [18–24]. Until 2010, after a series of strictly technical improvement on the NOPA system, the EPR entanglement degree was raised to $-6\ dB$ [25], which was the best reported result on NOPA system. In principle, according to the generally theoretical model without considering the influences of the extra phase noises on the anti-squeezing quadrature, the entanglement of the output field from a NOPA is limited fundamentally only by its escape efficiency (the ratio of the transmissivity efficiency to the sum of the transmissivity efficiency and the intra-cavity loss) and the pump parameter (the ratio of the pump power to the pump threshold). For a given NOPA with certain escape efficiency, we could raise the entanglement by increasing the pump power. However, in the practical system there always are unavoidable extra phase noises and the thermal effect of the nonlinear crystal, which increase along with the pump power. For keeping the stability of NOPA and degrading the influence of extra noises, usually the pump parameters are limited between 60 % and 75 %, which are the optimal pump parameters of each NOPA for producing the stable and possibly highest entanglement [12–16, 19, 20, 25].

For further raising entanglement under generally technical condition, we design the cascaded NOPA system involving three NOPAs and experimentally realized the cascaded amplification of CV entanglement. The initial EPR entanglement of $-5.3\ dB$ produced by the first NOPA (NOPA1) is enhanced to $-7.2\ dB$ by the second one (NOPA2) and successively to $-8.1\ dB$ by the third one (NOPA3), which is the highest EPR entanglement of optical modes obtained by experiments so far to the best of our knowledges. We numerically calculate the correlation variances of the enhanced EPR entangled state based on the physical parameters of the experimental system. The calculated results are in good agreement with the experimental measurements.

Fig.1 shows the principle schematic of the cascaded entanglement enhancement system. The laser source is an intra-cavity frequency-doubled CW laser, the output second-harmonic wave (ω_p) from which is used for the pump fields of the three NOPAs and the output fundamental wave ($\omega_{p/2}$) serves as the injected signal of NOPA1 and the local oscillator (LO) of the balanced homodyne detector (BHD) for the entanglement measurement. The EPR entangled light generated by NOPA1 (EPR1) is injected into NOPA2 as the injected signal for the first-stage enhancement of the entanglement and the the amplified EPR optical field (EPR2) is injected into NOPA3 for the second-stage enhancement. The final entangled light (EPR3) is detected by the BHD. Only when the three NOPAs are operated simultaneously at de-amplification situation or at amplification situation the cascaded entanglement enhancement can be achieved. Otherwise, the entanglement of the injected seed field will be degraded by the next NOPA operated at opposite situation [26, 27]. In the presented experiment, the three NOPAs are operated below the oscillation threshold of NOPA and at the de-amplification situation, i.e. the pump field and the injected signal are out of phase (with the phase difference of $(2n+1)\pi$, n-integer). In this case the produced entangled states have the correlated amplitude-sum and phase-difference as well as the anti-correlated amplitude-difference and phase-sum [19–21].

In the following we calculate the correlation variances between the amplitude and phase quadratures of the EPR entangled state enhanced by a NOPA firstly. We describe the quantum state of light with the electromagnetic field annihilation operators $\hat{a} = (\hat{X} + i\hat{Y})/2$, where $\hat{X}$ and $\hat{Y}$ are the operators of the amplitude ($\hat{X}$) and the phase ($\hat{Y}$) quadratures, respectively. $\hat{X}$ and $\hat{Y}$ satisfy the canonical commutation relation $[\hat{X}, \hat{Y}] = 2i$. The correlation variances and the anti-correlation variances of the injected EPR optical modes which is produced by the former NOPA, are expressed by $\langle \delta^2(\hat{X}^{in}_{a_1} + \hat{X}^{in}_{a_2})\rangle = \langle \delta^2(\hat{Y}^{in}_{a_1} - \hat{Y}^{in}_{a_2})\rangle = 2e^{-2r}$ and $\langle \delta^2(\hat{X}^{in}_{a_1} - \hat{X}^{in}_{a_2})\rangle = \langle \delta^2(\hat{Y}^{in}_{a_1} + \hat{Y}^{in}_{a_2})\rangle = 2e^{2r+2r'}$, where r and r' are the correlation parameter and the extra noise factor on the anti-correlation components, respectively; $\hat{X}^{in}_{a_{1(2)}}$ and $\hat{Y}^{in}_{a_{1(2)}}$ stand for the amplitude and the phase quadratures of the injected mode $\hat{a}^{in}_{1(2)}$, respectively [26, 28]. Here, we have supposed that the signal and idler modes are balanced which is easily satisfied in experiment [18–21]. Solving the quantum Langevin motion equations and using the input-output relation of the NOPA, the correlation variances of the output field are obtained:

$$
\begin{aligned}
&\langle\delta^2(\hat{X}^{out}_{a_1}+\hat{X}^{out}_{a_2})\rangle = \langle\delta^2(\hat{Y}^{out}_{a_1}-\hat{Y}^{out}_{a_2})\rangle \\
&= (\zeta(2\frac{(-\kappa+\gamma_1-\gamma_2)^2+(\omega\tau)^2}{(\kappa+\gamma_1+\gamma_2)^2+(\omega\tau)^2}e^{-2r} \\
&\quad +\frac{8\gamma_1\gamma_2}{(\kappa+\gamma_1+\gamma_2)^2+(\omega\tau)^2}) + 1-\zeta)\cos^2\theta \\
&\quad +(\zeta(2\frac{(-\kappa+\gamma_1-\gamma_2)^2-(\omega\tau)^2}{(\kappa+\gamma_1+\gamma_2)^2+(\omega\tau)^2}e^{2r+2r'} \\
&\quad +\frac{8\gamma_1\gamma_2}{(\kappa+\gamma_1+\gamma_2)^2+(\omega\tau)^2}) + 1-\zeta)\sin^2\theta, \qquad (1)
\end{aligned}
$$

where $\hat{X}^{out}_{a_{1(2)}}$ and $\hat{Y}^{out}_{a_{1(2)}}$ are the amplitude and the phase quadratures of the output mode $\hat{a}^{out}_{1(2)}$, respectively; γ_1 and γ_1 are the transmissivity efficiency and the intra-cavity loss of the NOPA; $\kappa = \beta\chi$ is the nonlinear coupling efficiency of the NOPA which is proportional to the pump parameter $\beta = (p_{pump}/p_{th})^{1/2}$ (p_{pump} - the pump power, p_{th} - the threshold pump power of NOPA) and the second-order nonlinear coupling coefficient χ of the nonlinear crystal used in the NOPA; τ is the round-trip time of light in the optical cavity; $\omega = 2\pi\Omega$ is the noise analysis frequency; ζ is the imperfect detection efficiency; and θ is the relative phase fluctuation between the pump field and the injected signal resulting from imperfect phase-locking.

Fig. 2 (a) is the calculated dependence of correlation variances of the output EPR optical field from NOPA3 on the cavity parameter γ_1 and γ_2, where other parameters are taken according to the really experimental system ($r = 0.83$; $r' = 0.45$; which correspond to the entanglement degree of EPR2 with correlation variance of -7.2 dB below the QNL and the anti-correlation variance of 11.1 dB above the QNL, see the experimental results in the text; $\theta = 0.0105; \Omega = 2.0\ MHz; \tau = 2.0 * 10^{-9}\ s; \varsigma = 0.947$.). When γ_1 increases and γ_2 decreases the correlation variance of the output field reduces, i.e. the entanglement degree increases. It means that for a simple NOPA the higher input-output transmissivity (γ_1) and the lower intra-cavity loss (γ_2) can provide the stronger performance of the entanglement enhancement. However, for a NOPA with given physical parameters, the correlation variances of the output field depend on the correlation variances of the injected signal field. Fig. 2 (b) shows the functions of the correlation variances of the output field vs that of the input field, where the trace (i) for $\gamma_1 = 0.1$, $\gamma_2 = 0.004$ and the trace (ii) for $\gamma_1 = 0.1$, $\gamma_2 = 0.001$; other parameters are the same as that of Fig. 2 (a). We can see from Fig. 2 (b), there is a turning point in the trace (i) ($-8.5\ dB$) and (ii) ($-10.0dB$), respectively, where the correlation variance of the output field equals to that of the input field. After the turning

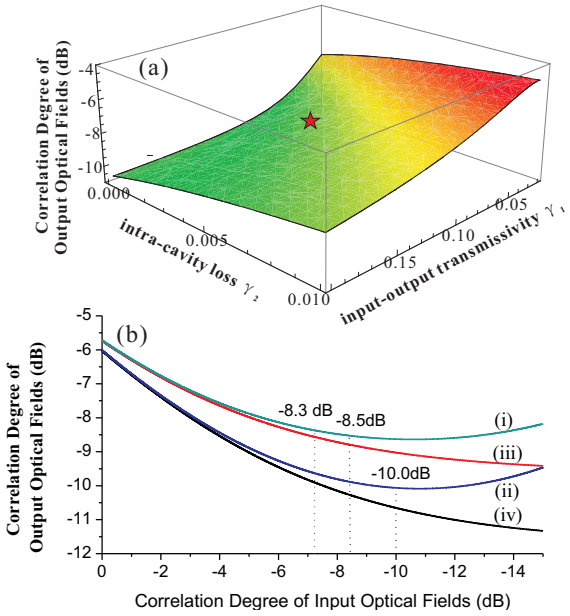

FIG. 2. (Color online) (a) The dependence of correlation variances of the output entangled optical field on the input-output transmissivity γ_1 and the intra-cavity loss γ_2 of NOPA. (b) The functions of the correlation variances of the output field vs that of the input field for two NOPAs: (i) $\gamma_1 = 0.1$, $\gamma_2 = 0.004$, $\theta = 0.0105$; (ii) $\gamma_1 = 0.1$, $\gamma_2 = 0.001$, $\theta = 0.0105$; (iii) $\gamma_1 = 0.1$, $\gamma_2 = 0.004$, $\theta = 0$; (iv) $\gamma_1 = 0.1$, $\gamma_2 = 0.001$, $\theta = 0$.

point the correlation variances of the output field will be larger than that of the input signal. It means the enhancement ability of the NOPA no longer exists. Comparing traces (i) and (ii), it is obvious that the NOPA with the smaller intra-cavity loss (trace (ii)) has stronger ability of the entanglement enhancement. This is because the noises of the anti-correlation components in the input field increase rapidly along with the increasing of the correlation degree, and the noises on the anti-correlation components would be inevitably coupled to the correlation component and thus decrease the correlation degree of the output fields due to the existence of the phase fluctuation θ in the experimental system (See the second term of Eq. (1)). Reducing the phase fluctuation in the phase-locking system, the upper limitation of the input field for the entanglement enhancement will be raised. For the ideal case of $\theta = 0$ the turning point will vanish [See curves (iii) and (iv) of Fig. 3(b)].

The experimental setup is shown in Fig.3. A continuous-wave intra-cavity frequency-doubled and frequency-stabilized Nd:YAP/LBO (Nd-dropped $YAlO_3/LiB_3O_5$) laser (Yuguang Co. Ltd., FG-VIB) with both the harmonic-wave output at $540\ nm$ and the subharmonic-wave output at

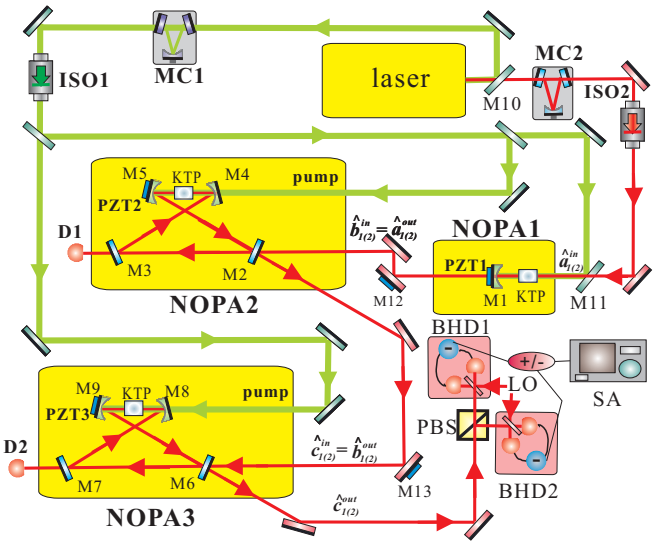

FIG. 3. (Color online) The experimental setup of cascade sensitive-phase entanglement enhancement. laser, Nd:YAP/LBO laser source; PBS, polarizing beam splitter; MC1(2), mode cleaner; ISO1(2), optical isolator; M0–M13, different mirrors (see text for details); PZT, piezoelectric transducer; D1(2), photo detector; +/-, positive/negative power combiner; SA, spectrum analyzer.

$1080\ nm$ serves as the laser source of the entanglement enhancement system. The output green and infrared lasers are separated by a beam splitter M10 coated with high reflection for $540\ nm$ and high transmission for $1080\ nm$. The green laser serves as the pump fields of three NOPAs and the infrared laser is used for the injected signal of NOPA, as well as the local oscillators (LO) of BHD1 and BHD2. The traveling-wave mode cleaners (MC1 for $540\ nm$ and MC2 for $1080\ nm$) consisting of three mirrors are used for the optical low-pass filters of noises and the spatial mode cleaners. The finesses of MC1 for $540\ nm$ and MC2 for $1080\ nm$ both are 550. The optical isolators (ISO1 for $540\ nm$ and ISO2 for $1080\ nm$) are utilized to prevent the feedback optical fields from the NOPA returning to the laser. We choose the α-cut Type II KTP ($KTiOPO_4$) to be the nonlinear mediums in the three NOPAs, which can achieve type-II noncritical phase-matched frequency-down-conversion of the pump field at 1080 nm. The size of the three KTP crystals is the same ($3*3*10mm^3$) and temperature of the KTP crystal in the three NOPAs is controlled around $63°C$ to satisfy the phase-matching condition. Since the phase-matching temperature of KTP has a broad full width of about $30°C$, we can make the signal and the idler modes double-resonating inside a NOPA by carefully tuning the temperature of the crystal around $63°C$. The NOPA1 is in a semi-monolithic Fabry-Perot configuration consisting of a KTP crystal and a concave mirror

(M1) with $50\ mm$ radius of curvature. The front face of the crystal is coated to be used as the input coupler of the pump field (the transmissivity of 99.8% at $540\ nm$ and 0.04% at $1080\ nm$), and the other face is coated with the dual-band antireflection at both $540\ nm$ and $1080\ nm$. M1 coated with transmissivity of 5.2% at $1080\ nm$ and high reflection at $540\ nm$ is used as the output coupler and is mounted on a piezoelectric transducer (PZT1) to scan actively the cavity length of NOPA1 or lock it on resonance with the injected signal as needed. However, due to the existence of the unavoidable extra phase noises the relative phase between the pump field and the injected seed light is not able to be locked at the required value (0 or π) exactly and there always is a phase fluctuation θ around the locked value. The value of θ can be experimentally detected by measuring the rms noise of the error signals on locked operation [29]. The length and the finesse of the cavity of NOPA1 are $54\ mm$ and 115, respectively. The NOPA2 (3) has the ring configuration consisting of two flat mirrors M2 (6) and M3 (7) and two concave mirrors M4 (8) and M5 (9) with $100\ mm$ radius of curvature. The KTP crystal with the $1080\ nm$ and $540\ nm$ dual-band antireflection coated at both end faces is placed in the middle of M4 (8) and M5 (9). M2 (6) serves as the input-output coupler with the transmission of 10.0% at $1080\ nm$ and antireflection at $540\ nm$, respectively. All the other mirrors are high reflection at $1080\ nm$ and antireflection at $540\ nm$. M5 (9) is mounted on PZT2 (3) for scanning or locking actively the length of the optical cavity NOPA2 (3). The length and the finesse of the cavity for both NOPA2 and NOPA3 are $557\ mm$ and 60, respectively. The threshold pump powers of the three NOPAs are $250\ mW$ for NOPA1 and $900\ mW$ for NOPA2 and NOPA3, respectively. To lock the relative phase between the injected seed and the pump light of NOPA2 (3) to the de-amplification point we phase-modulate the seed light using a dither signal of 37kHz (41kHz) by means of the PZT mounted on M12 (13). Then we monitor the intensity of the leaked seed light from the cavity mirror M3 (7) with the photo detector D1 (D2) and make the intensity to the minimum, i.e. the relative phase equals π by controlling the PZT on M12 (13). In this case, we demodulate the modulated dither signal on the output of D1 (2) and feedback the error signal to the PZT on M12 (13) to lock the parametric gain of NOPA2 (3) at the de-amplification point. However, there is always the phase fluctuation in real experiments which will unavoidably influence the phase-locking precision. The measured fluctuation of θ around π is about 0.0105 for our experimental system. From the second term of Eq. (1) we can see that the influence of the θ fluctuation to the entanglement enhancement depends on the entanglement degree of the injected seed light. The higher the initial entanglement is, the stronger the influence is. The signal and the idler optical beams with orthogonal polarizations produced by NOPA3 are separated by

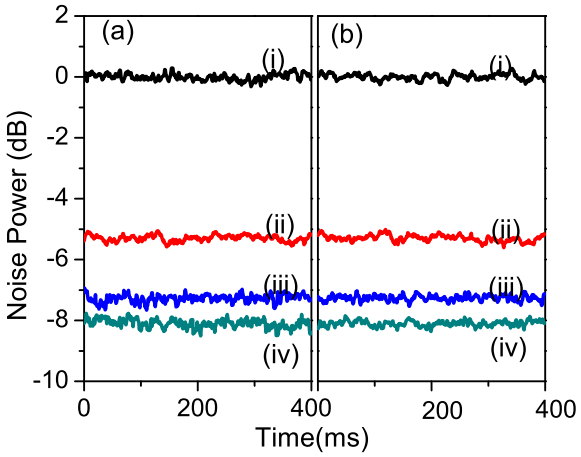

FIG. 4. (Color online) Noise powers of the correlation variances: (a) Trace (i), the QNL; trace (ii), correlation variance of $\langle\delta^2(\hat{X}^{out}_{a_1}+\hat{X}^{out}_{a_2})\rangle$; trace (iii), correlation variance of $\langle\delta^2(\hat{X}^{out}_{b_1}+\hat{X}^{out}_{b_2})\rangle$; trace (iv), correlation variance of $\langle\delta^2(\hat{X}^{out}_{c_1}+\hat{X}^{out}_{c_2})\rangle$. (b) Trace (i), The QNL; trace (ii), correlation variance of $\langle\delta^2(\hat{Y}^{out}_{a_1}-\hat{Y}^{out}_{a_2})\rangle$; trace (iii), correlation variance of $\langle\delta^2(\hat{Y}^{out}_{b_1}-\hat{Y}^{out}_{b_2})\rangle$; trace (iv), correlation variance of $\langle\delta^2(\hat{Y}^{out}_{c_1}-\hat{Y}^{out}_{c_2})\rangle$.

a polarizing-beam-splitter (PBS) and then are detected by BHD1 and BHD2, respectively. The BHD consists of a $50/50$ beam-splitter and a pair of photodiodes (ETX-500 InGaAs). Locking the relative phase between the signal (idler) beam and the LO to 0 or $\pi/2$, the fluctuations of amplitude or phase quadrature of the signal (idler) field can be measured by BHD1 (2). The noise powers of the amplitude (phase) quadratures simultaneously measured by BHD1 and BHD2 are combined by the positive (negative) power combiner ($\oplus(\ominus)$) and then the correlation variances of the amplitude-sum (phase-difference) are analyzed by a spectrum analyzer (SA).

Figs. 4 (a) and (b) show the measured correlation variances of the amplitude-sum and the phase-difference, respectively. In Fig. 4 (a) [(b)] trace (i) is the QNL, trace (ii), (iii) and (iv) are the measured noise power spectra of the amplitude-sum (phase-difference) at 2 MHz for EPR1, EPR2 and EPR3, respectively. The initial correlation variances of EPR1 produced by NOPA1 are $\langle\delta^2(\hat{X}^{out}_{a_1}+\hat{X}^{out}_{a_2})\rangle = \langle\delta^2(\hat{Y}^{out}_{a_1}-\hat{Y}^{out}_{a_2})\rangle = 0.59$, corresponding to $-5.3\pm0.2\ dB$ below the QNL. After the first-stage enhancement by NOPA2 the correlation variances are reduced to $\langle\delta^2(\hat{X}^{out}_{b_1}+\hat{X}^{out}_{b_2})\rangle = \langle\delta^2(\hat{Y}^{out}_{b_1}-\hat{Y}^{out}_{b_2})\rangle = 0.38$, corresponding to $-7.2\pm0.2\ dB$ below the QNL. At last, after the cascaded enhancement by NOPA2 and NOPA3, the correlation variances

of EPR3 become $\langle\delta^2(\hat{X}^{out}_{c_1}+\hat{X}^{out}_{c_2})\rangle = \langle\delta^2(\hat{Y}^{out}_{c_1}-\hat{Y}^{out}_{c_2})\rangle = 0.31$, corresponding to -8.1 ± 0.2 dB below the QNL. The correlation variance of EPR3 is denoted in Fig. 2 (a) with a red star, where $\gamma_1 = 0.1$, $\gamma_2 = 0.004$, $r = 0.83$, (-7.2 dB below the QNL) corresponding to the operation conditions of NOPA3. On the trace (i) of Fig. 2 (b) we can see, when the correlation variance of the input EPR beam (EPR2) equals to -7.2 dB, the correlation variance of the output field (EPR3) is -8.3 dB which is in good agreement with the experimental measured value (-8.1 dB). We also measured the anti-correlation variances of EPR1, EPR2 and EPR3, which are $\langle\delta^2(\hat{X}^{out}_{a_1}-\hat{X}^{out}_{a_2})\rangle = \langle\delta^2(\hat{Y}^{out}_{a_1}+\hat{Y}^{out}_{a_2})\rangle = 13.6$, $\langle\delta^2(\hat{X}^{out}_{b_1}-\hat{X}^{out}_{b_2})\rangle = \langle\delta^2(\hat{Y}^{out}_{b_1}+\hat{Y}^{out}_{b_2})\rangle = 25.9$, and $\langle\delta^2(\hat{X}^{out}_{c_1}-\hat{X}^{out}_{c_2})\rangle = \langle\delta^2(\hat{Y}^{out}_{c_1}+\hat{Y}^{out}_{c_2})\rangle = 34.2$ corresponding to 8.3 dB, 11.1 dB and 12.3 dB above the QNL, respectively. The sums of the amplitude and the phase correlation variances for EPR1, EPR2 and EPR3 are 1.18, 0.76, and 0.62, respectively, all of which satisfy the inseparability criterion, i.e. these values are smaller than 4(when the sum is larger than 4 the signal and the idler optical modes in the output field are separable and thus do not form an entangled state) [8, 9].

In conclusion, we have experimentally demonstrated that the CV entanglement of optical field can be enhanced by the cascaded NOPA. The upper limitation of the enhanced entanglement depends on the intra-cavity loss (γ_2) of the NOPA and the relative phase fluctuation θ of the phase locking system. The presented scheme opens an avenue to enhance CV entanglement using easily reachable optical devices. Besides, the presented cascaded system perhaps can be used as a part of a particular quantum information protocol, where the entanglement needs to be successively enhanced step by step, which could be an open question for further study.

This research was supported by National Basic Research Program of China (Grant No. 2010CB923103), Natural Science Foundation of China (Grants Nos. 60736040, 11074157 and 61121064), the TYAL.

[1] A. Galindo, and M. A. Martin-Delgado, Rev. Mod. Phys. **74**, 347 (2002).

[2] S. L. Braunstein, and P. van Loock, Rev. Mod. Phys. **77**, 513 (2005).

[3] M. D. Reid et al., Rev. Mod. Phys. **81**, 1727 (2009).

[4] D. Bouwmeester et al., Nature (London) **390**, 575 (1997).

[5] A. Furusawa et al., Science **282**, 706709 (1998).

[6] A. Einstein, B. Podolsky, and N. Rosen, Phys. Rev. **47**, 777 (1935).

[7] M. D. Reid, Phys. Rev. A **40**, 913 (1989).

[8] L. M. Duan, G. Giedke, J. I. Cirac, and P. Zoller, Phys. Rev. Lett. **84**, 2722 (2000).

[9] R. Simon, Phys. Rev. Lett. **84**, 2726 (2000).

[10] L. A. Wu, H. J. Kimble, J. L. Hall, and H. Wu, Phys. Rev. Lett. **57**, 2520 (1986).

[11] A. M. Lance, T. Symul, W. P. Bowen, B. C. Sanders, and P. K. Lam , Phys. Rev. Lett. **92**, 177903 (2004).

[12] Y. Takeno, M. Yukawa, H. Yonezawa, and A. Furusawa, Opt. Express, **15**, 4321 (2007).

[13] T. Eberle et al., Phys. Rev. Lett. **104**, 251102 (2010).

[14] M. Mehmet et al., Phys. Rev. A **81**, 013814 (2010).

[15] M. Mehmet et al., Opt. Express **19**, 25763 (2011).

[16] T. Eberle et al., Phys. Rev. A **83**, 052329 (2011).

[17] M. Yukawa, R. Ukai, P. van Loock, and A. Furusawa, Phys. Rev. A **78**, 012301 (2008).

[18] Z. Y. Ou, S. F. Pereira, H. J. Kimble, and K. C. Peng, Phys. Rev. Lett. **68**, 3663 (1992).

[19] X. Y. Li et al., Phys. Rev. Lett. **88**, 047904 (2002).

[20] X. J. Jia et al., Phys. Rev. Lett. **93**, 250503 (2004).

[21] J. Laurat, T. Coudreau, G. Keller, N. Treps, and C. Fabre , Phys. Rev. A **71**, 022313 (2005).

[22] A. S. Villar, L. S. Cruz, K. N. Cassemiro, M. Martinelli, and P. Nussenzveig, Phys. Rev. Lett. **95**, 243603 (2005).

[23] J. T. Jing, S. Feng, R. Bloomer, and O. Pfister, Phys. Rev. A **74**, 041804 (2006).

[24] G. Keller et al., Opt. Express **16**, 9351 (2008).

[25] Y. Wang et al., Opt. Express **18**, 6149 (2010).

[26] H. X. Chen, and J. Zhang, Phys. Rev. A **79**, 063826 (2009).

[27] Y. N. Shang, X. J. Jia, Y. M. Shen, C. D. Xie, and K. C. Peng, Opt. Lett. **35**, 853 (2010).

[28] J. Zhang, C. D. Xie and K. C. Peng, Phys. Lett. A **299**, 427 (2002).

[29] T. C. Zhang, K. W. Goh, C. W. Chou, P. Lodahl, and H. J. Kimble, Phys. Rev. A **67**, 033802 (2003).